

We are IntechOpen, the world's leading publisher of Open Access books Built by scientists, for scientists

6,900

Open access books available

186,000

International authors and editors

200M

Downloads

Our authors are among the

154

Countries delivered to

TOP 1%

most cited scientists

12.2%

Contributors from top 500 universities



WEB OF SCIENCE™

Selection of our books indexed in the Book Citation Index
in Web of Science™ Core Collection (BKCI)

Interested in publishing with us?
Contact book.department@intechopen.com

Numbers displayed above are based on latest data collected.
For more information visit www.intechopen.com



Breast Ultrasound Tomography

Nebojsa Duric and Peter Littrup

Additional information is available at the end of the chapter

<http://dx.doi.org/10.5772/intechopen.69794>

Abstract

Both mammography and standard ultrasound (US) rely upon subjective criteria within the breast imaging reporting and data system (BI-RADS) to provide more uniform interpretation outcomes, as well as differentiation and risk stratification of associated abnormalities. In addition, the technical performance and professional interpretation of both tests suffer from machine and operator dependence. We have been developing a new technique for breast imaging that is based on ultrasound tomography which quantifies tissue characteristics while also producing 3-D images of breast anatomy. Results are presented from clinical studies that utilize this method. In the first phase of the study, ultrasound tomography (UST) images were compared to multi-modal imaging to determine the appearance of lesions and breast parenchyma. In the second phase, correlative comparisons with MR breast imaging were used to establish basic operational capabilities of the UST system. The third phase of the study focused on lesion characterization. Region of interest (ROI) analysis was used to characterize masses. Our study demonstrated a high degree of correlation of breast tissue structures relative to fat subtracted contrast-enhanced MRI and the ability to scan ~90% of the volume of the breast at a resolution of 0.7 mm in the coronal plane.

Keywords: breast, ultrasound, 3-D imaging, tomography, cancer

1. Introduction

Breast cancer is the most common cancer among women, accounting for one-third of cancers diagnosed. Statistically, ~230,000 new cases of invasive breast cancer and ~63,000 in situ breast carcinomas are diagnosed in the US annually; breast cancer is the third leading cause of cancer death among women, causing ~40,000 deaths in the US every year [1]. According to SEER statistics, approximately 61% of women are found to have localized breast cancers at the time of diagnosis; about 31% are found to be regional disease; another 5% are diagnosed with distant metastases while about 3% are unstaged [2]. The 5-year survival rate for women with localized

cancer is 98%; for those with regional disease, it drops to 84%; for those diagnosed with distant stage, the survival rate drops dramatically to 23%; while for unstaged cancers the 5-year survival rate is about 58%. **Figure 1** illustrates the dependence of survival on cancer stage.

There are many reasons why cancers are not detected early but some of the major factors relate to limited participation in breast screening and the performance of screening mammography.

1.1. Limited participation in screening

National cancer screening statistics indicate that only 51% of eligible women undergo annual mammograms [4]. That rate is even lower for African American women and/or those of lower socioeconomic groups. Access, fear of radiation and discomfort are some of the factors that contribute to the low participation rate. Greater participation would lead to detection of breast cancer at an earlier stage leading to longer survival. Increased participation and improved breast cancer detection would have the greatest effect on the statistic of nearly 1 in 3 women who are diagnosed each year with later stage (regional or greater) breast cancer, totaling approximately 60,000 women per year in the USA. The net effect would be an increase in survival time and a corresponding decrease in mortality rates. This is also suggested in a recent meta-analysis, whereby increased participation and sensitivity lead to additional invasive cancer detection and greater mortality reduction [4].

1.2. Limited performance of mammography

For women with dense breast tissue, who are at the highest risk for developing breast cancer [5–8], the performance of mammography is at its worst [9]. Consequently, many cancers are

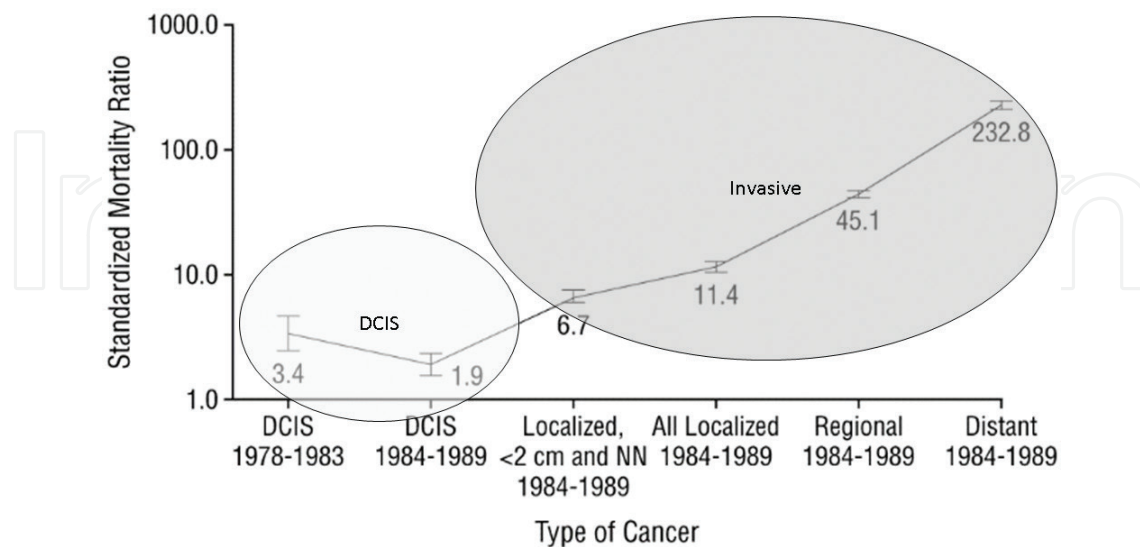


Figure 1. The dependence of mortality rates on cancer type and stage. From Kerlikowske et al. [3].

missed at their earliest stages when they are the most treatable. Improved cancer detection for women with denser breasts would decrease the proportion of breast cancers diagnosed at later stages, which would significantly lower the mortality rate.

1.3. The breast screening challenge

X-ray mammography detects about 5 cancers per 1000 screens [10]. However, its positive predictive value (PPV) is low and its sensitivity is greatly reduced in women with dense breast tissue [10]. Although digital breast tomosynthesis (DBT) may improve upon some of the limitations of standard mammography, it is unlikely to create a paradigm shift in performance [11] while generating even higher levels of ionizing radiation [12]. MRI can significantly improve on these limitations by virtue of its volumetric, radiation-free imaging capability. Studies have shown that MRI can have a positive impact in the breast management continuum ranging from risk assessment to diagnosis and treatment monitoring [12, 13]. However, MRI can have a high false positive rate, requires contrast injection and the exams can be both long and costly [14]. Furthermore, MR has long been prohibitively expensive for routine use and there is a need for a low-cost equivalent alternative. Yet, for high-risk women, MRI is now viewed as the gold standard for breast cancer detection and screening [15–23]. Positron emission tomography is also limited by cost and radiation concerns.

Recent studies have demonstrated the effectiveness of hand held ultrasound imaging in detecting breast cancer, particularly for women with dense breasts (**Table 1**). These studies have shown that up to 4.5 extra cancers were detected per 1000 screens [24–34]. A striking aspect of the added detections is that they are predominantly node negative invasive cancers which would have potentially progressed to a later stage before possible mammographic detection. Moreover, there is little risk of over detection of ductal carcinoma in situ (DCIS). The sensitivity of mammography is greater for DCIS than it is for invasive cancer, with DCIS making up approximately 25% of mammographic screen-detected breast cancers [35].

We have examined the data from these studies to extract the statistics of cancer detection by imaging mode (**Table 1**). The results are summarized in **Figure 2**. It is striking to note that ultrasound (US) almost doubles the cancer detection rate in dense breasts. However, despite these successful study outcomes, handheld ultrasound is unlikely to be adopted for screening because it is operator dependent, and its imaging aperture is small, which hinders whole breast imaging. Furthermore, ultrasound's increased sensitivity to invasive cancer is offset by lowered sensitivity to DCIS by virtue of mammography's greater ability to detect microcalcifications. Although such a trade-off may be justified by the fact that mortality from invasive cancers is much higher than that from DCIS, a combined screening [mammography plus automated breast ultrasound (ABUS)] would provide a comprehensive screen. It has therefore been proposed that ABUS be used for screening, supplemental to mammography.

Author (Year)	Center	Type	Exams	US only cancers	Yield per 1000
Brem et al. (2014)	Multi	ABUS	15,318	30	1.96
Berg et al. (2012)	Multi	HHUS	7473	32	4.28
Hooley et al. (2012)	Single	HHUS	935	3	3.21
Kelly et al. (2010)	Multi	AWBU	6425	23	3.58
Corsetti et al. (2008)	Multi	HHUS	9157	37	4.04
Crystal et al. (2003)	Single	HHUS	1517	7	4.61
Leconte et al. (2003)	Single	HHUS	4236	16	3.78
Kolb et al. (2002)	Single	HHUS	13,547	37	2.73
Kaplan (2001)	Single	HHUS	1862	6	3.22
Buchberger et al. (2000)	Single	HHUS	8103	32	3.95
Gordon et al. (1995)	Single	HHUS	12,706	44	3.46

Table 1. Summary of studies used in the analysis.

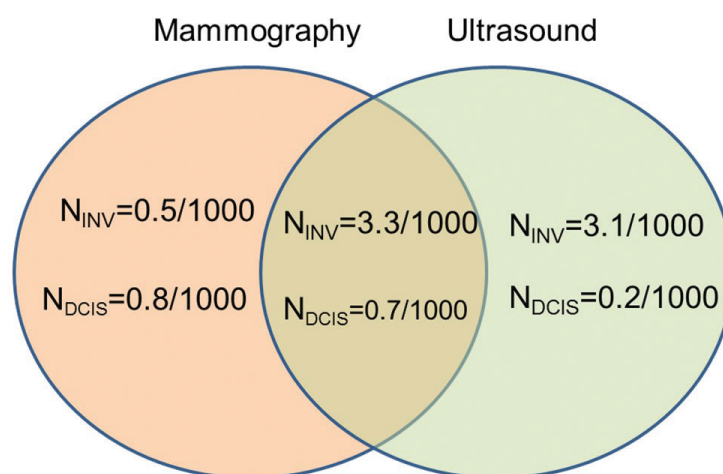


Figure 2. Venn diagram summarizing comparative cancer detection rates for screening mammography and ultrasound.

To that end, automated breast ultrasound (ABUS) has been introduced as a way of overcoming these issues, mainly by reducing operator dependence and increasing the field of view. For example, the GE Invenia ABUS ultrasound system for breast cancer screening, originally developed by U-Systems., recently received screening approval, adjunctive to mammography, from the FDA, because it demonstrated an ability to detect cancers missed by mammography in dense breasts. The SomoInsight screening study [24], indeed showed that ABUS plus mammography outperformed mammography alone, leading to the first FDA approval for ultrasound screening for breast cancer.

The fundamental quandary of breast screening today is the knowledge that (i) mammography misses cancers in dense breasts, (ii) that Automated Breast ultrasound (ABUS) detects cancers that mammography misses and yet (iii) screening continues largely with mammography only. This paradox

is amplified even further by the proliferation of state breast density notification laws in the USA which mandate that this information be available to women undergoing breast cancer screening. The primary reason this paradox exists today is that ABUS screening increases call back rates (up to a factor of two in case of the SomoInsight study [23]). The improvement in classification performance, measured by the area under the ROC curve, is modest because the increase in sensitivity is partially offset by an increase in false positives thus slowing its adoption. Technically, with its basic B-mode capability, ABUS has the same issue with false positives as hand held ultrasound. It is therefore unlikely that ABUS will be widely adopted for screening in the foreseeable future without more tissue-specific imaging capability. Improved lesion characterization would help lower the barriers to adoption of screening ultrasound.

1.4. Potential role of UST

Ultrasound tomography (UST) is an emerging technique that has the potential for tissue-specific imaging and characterization, by virtue of its transmission imaging capability [36–61]. Improved specificity would lower call back rates and lower the barriers to adoption. An adjunctive use of UST would have the potential to improve specificity relative to current ABUS and provide a comprehensive screen that would uncover invasive cancers otherwise missed by mammography. Detection of such early stage invasive cancers would provide women with curative treatment, the opportunity for which might be otherwise lost.

Conventional reflection ultrasound exploits differences in acoustic impedance between tissue types to provide anatomical images of breast tumors [62, 63]. However, reflection is just one aspect of a multi-faceted set of acoustic signatures associated with the biomechanical properties of tissue. UST is a technique that moves beyond B-mode imaging by virtue of its transmission capabilities. The latter provides additional characterization by measuring tissue parameters such as sound speed and attenuation (ATT) [64–68]. These parameters can be used to characterize lesions in a quantitative manner, a capability not available in current whole breast ultrasound systems. By merging reflection images with images of the bio-acoustic parameters of sound speed and attenuation, UST offers the possibility of exploiting differences in anatomical and physical properties of tissue to accurately differentiate cancer from normal tissue or benign disease. UST parameters are also quantitative, which allows new consideration of second and third-order statistical image analyses, or radiomics. Ultrasound has previously not been suitable for the burgeoning applications of radiomics due to its lack of true quantitative parameters such as sound speed (m/s) and attenuation (dB/cm/MHz). Initial assessments of UST performance was carried out, as described below.

In an initial attempt to assess the potential of UST in breast imaging, studies were carried out at the Karmanos Cancer Institute, Detroit, MI, USA. Informed consent was obtained from all patients, prospectively recruited in an IRB-approved protocol following HIPAA guidelines. Patients were scanned at the Alexander J Walt Comprehensive Breast Center. Standard multi-modality imaging was available for all patients. The Walt Breast Center houses SoftVue, a UST system manufactured by Delphinus Medical Technologies, Inc (Novi, MI). SoftVue embodies a number of attributes that differentiate it from conventional imaging modalities:

- *Water-based pulse coupling:* SoftVue utilizes a water filled imaging chamber that is kept at body temperature. Its primary purpose is to couple the sound energy between the transducer and the breast tissue.
- *Closed geometry probe:* A circular ring transducer surrounds the breast while both are immersed in water. There is no compression of the breast since the transducer is offset from the breast with water acting as the pulse coupling agent. The closed transducer geometry allows collection of signals that pass through the entire width of the breast, a requirement for transmission imaging and the reconstruction of sound speed and attenuation images. These parameters provide quantitative information in absolute units that are tied to external standards (km/s and dB/cm, respectively).
- *Operator independence:* Unlike mammography and other ABUS systems, multiple positionings are not required for larger breasts. Once the patient is positioned on the table, the operator simply presses the button and the exam is performed automatically without further intervention from the operator.
- *Scan time:* SoftVue scan time is 1–2 min per breast (depending on breast size). This scan duration minimizes intra-slice and inter-slice motion artifacts.
- *Image reconstruction time.* In this study, reconstruction time for a bilateral breast exam was ~30 min for the average patient and current hardware/software processing ability.

SoftVue was used to scan the recruited patients for this study. Coronal image series were produced by tomographic algorithms for reflection, sound speed and attenuation. All images were reviewed by a board-certified radiologist who has more than 20 years of experience in breast imaging and US-technology development. Symptomatic study participants were scanned with a SoftVue UST system. Pathological correlation was based on biopsy results and standard imaging (e.g. US definitive cyst).

Tomographic algorithms were used to generate images stacks of reflectivity, sound speed and attenuation for each patient. Lesions were identified based on correlation with standard imaging so that the tumor sound speed (SS) and attenuation (ATT) could be assessed. An example each type of image is shown in **Figure 3**.

In the first phase of the study, correlative comparisons with multi-modal imaging were carried out to assess lesion properties relative to mammography, US and MR. In the second

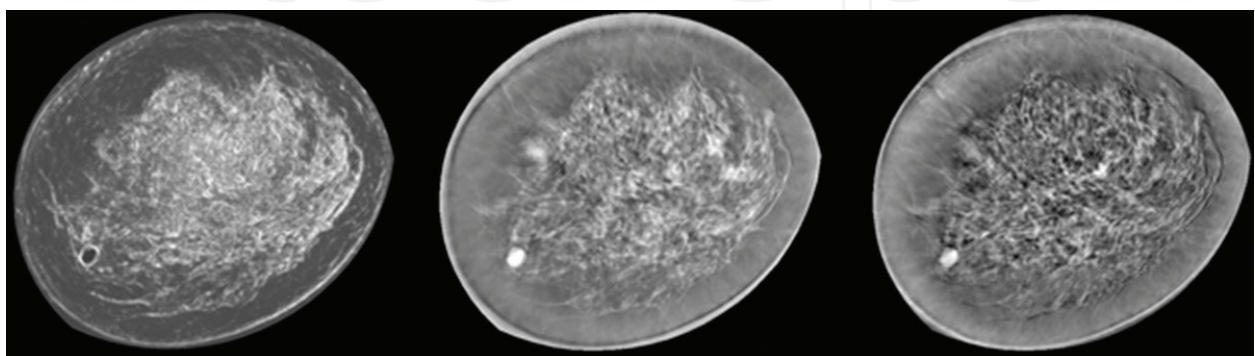


Figure 3. From left to right, reflection, sound speed and attenuation image slices depicting breast parenchyma and a fibroadenoma at 7 o'clock.

phase, MR breast imaging was used to establish basic operational capabilities of the UST system including the identification and characterization of parenchymal patterns, determination of the spatial resolution of UST and an estimate the breast volume that can imaged with UST. The third phase of the study focused on lesion characterization. Region of interest (ROI) analyses were performed on all identified lesions using all three UST image types. Combinations of the ROI generated quantitative values were used to characterize all masses, particularly in relation to relative differences with surrounding peritumoral regions.

2. Multi-modal comparisons

Since the patients were recruited at KCI on the basis of having a suspicious finding, standard imaging such as mammography, US and sometimes MRI were available, as well as the radiology and pathology reports. These images and the associated reports were used to retroactively locate the lesions in the UST image stacks for visual comparison. **Figures 4–7** show examples of UST images in relation to the other modalities. When MRI was available, the images were projected into the coronal plane for easier comparison with the UST whose native format is coronal.

Figure 4 shows a 9mm IDC at 3 o'clock. CC and MLO mammographic views of the affected breast are shown on the left with the lesion identified by arrows. The UST views corresponding

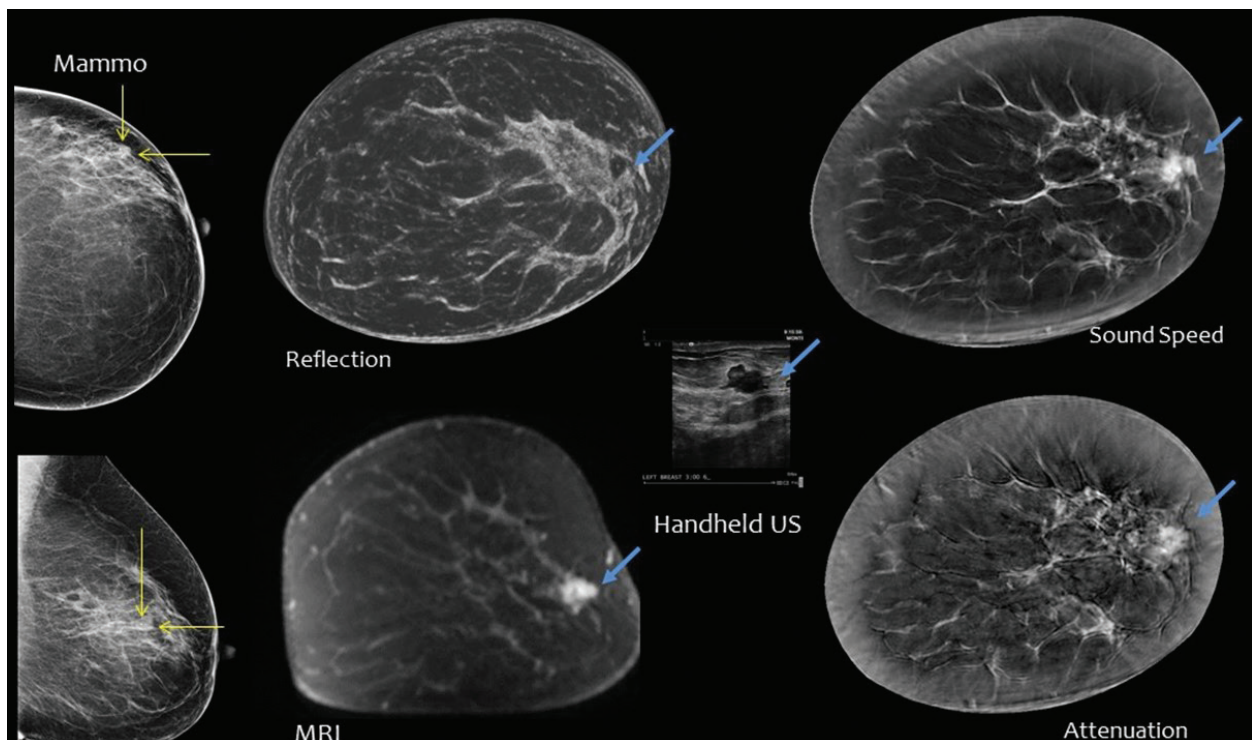


Figure 4. A 9 mm IDC at 3 o'clock. CC and MLO mammographic views of the affected breast are shown on the left with the lesion identified by arrows. The coronal UST views are shown in the form of reflection, sound speed and attenuation images. The corresponding ultrasound and MR images are also shown.

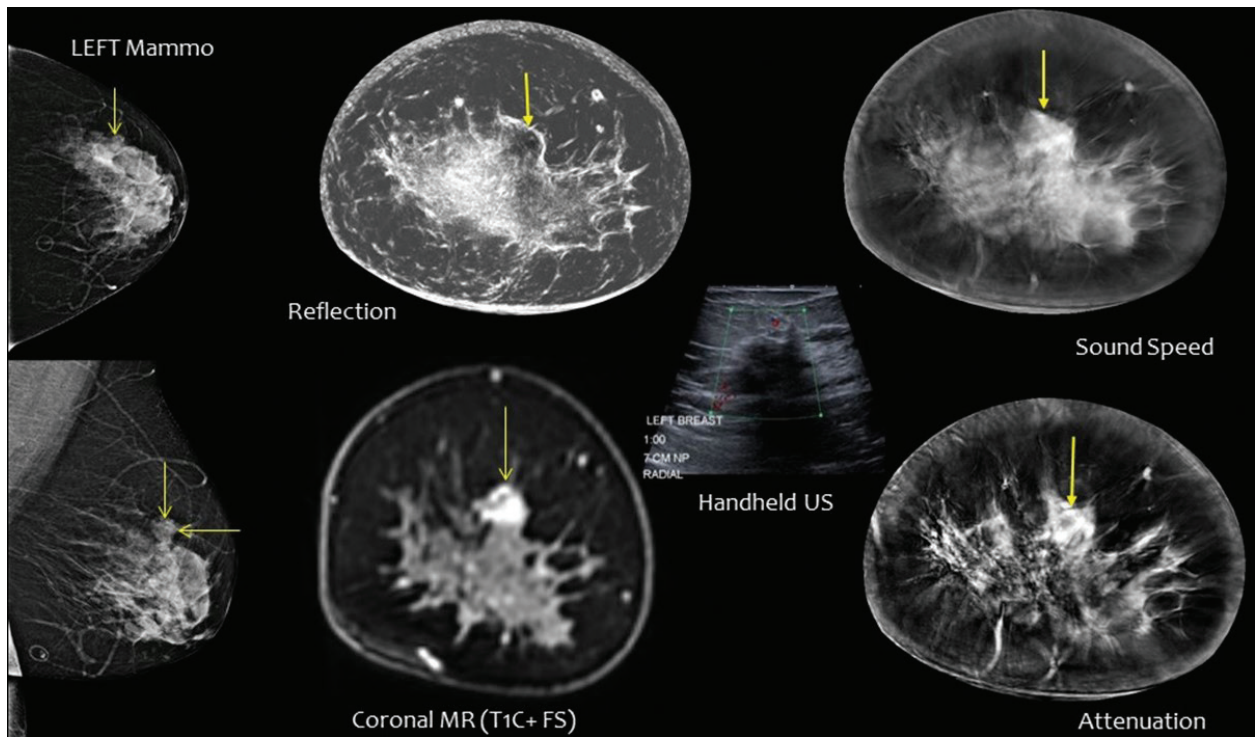


Figure 5. Multimodality images compared to UST reflection, sound speed and attenuation. An IDC is shown at 12 o'clock.

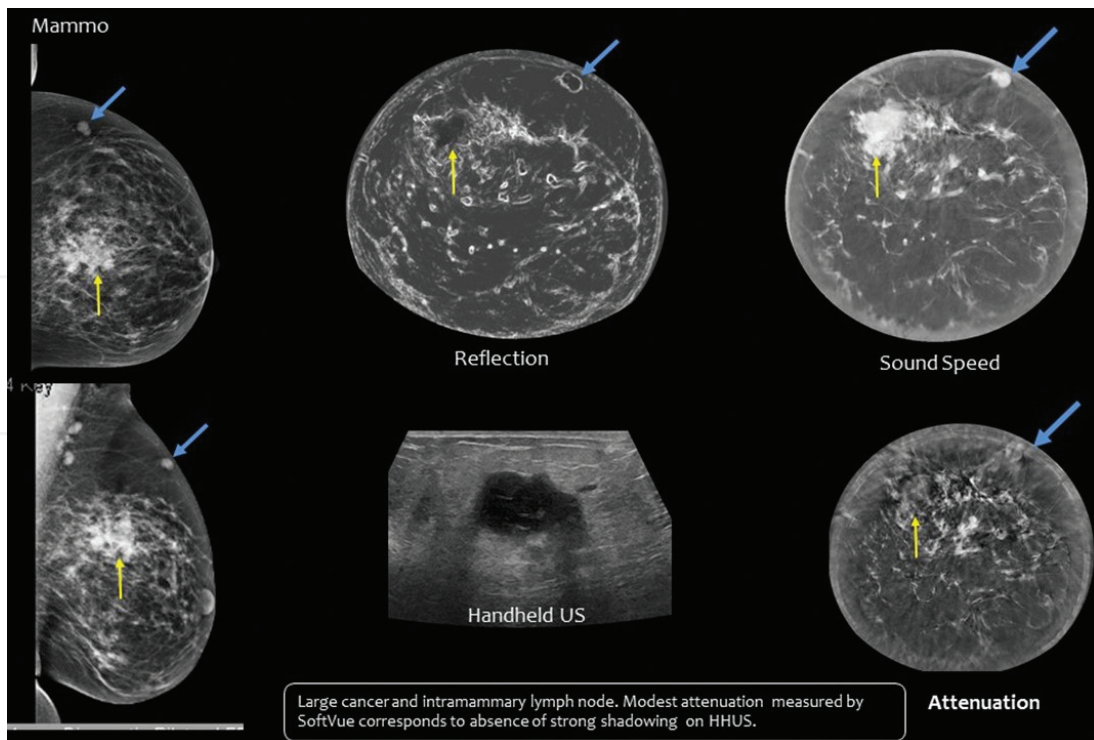


Figure 6. Multimodality images vs UST reflection, sound speed and attenuation showing an IDC and intramammary lymph node.

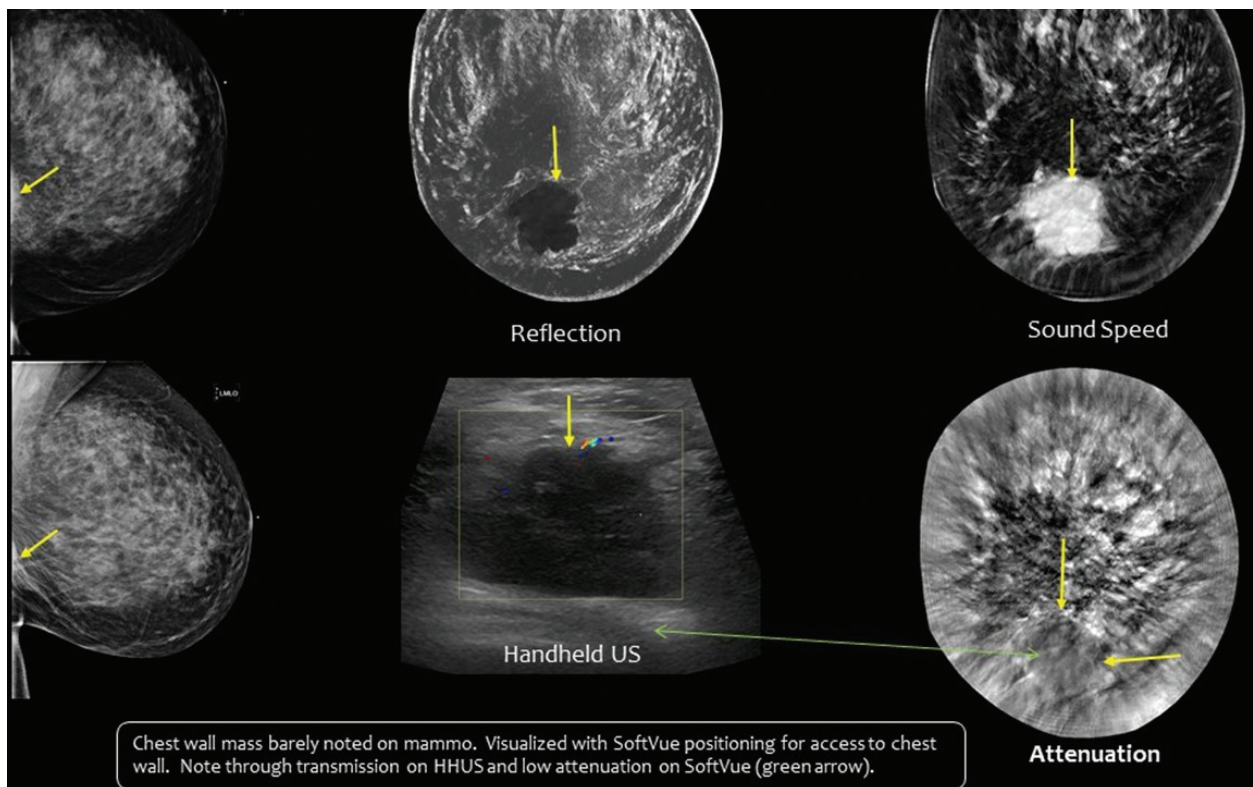


Figure 7. Illustrating the chest wall access achievable by UST relative to mammography.

to the coronal planes that contain the lesions are across the top with reflection, sound speed and attenuation images laid out from left to right. The corresponding ultrasound and MR images are shown along the bottom. Inspection of the images shows good correspondence in shape and location of the lesion. The greatest similarity is between the UST images and MRI. The IDC is seen to be hypoechoic in reflection and has high sound speed and attenuation contrast. An IDC in a heterogeneously dense breast is shown in **Figure 5** This IDC was initially missed by mammography. A large IDC and an intramammary lymph node are shown in **Figure 6**. Note the concordance between the UST images and mammography. **Figure 7** illustrates the chest wall access achievable by UST relative to mammography. Although UST does not access the entire axilla it does visualize the cancer that has invaded the chest wall.

3. MR concordance

UST and MR imaging was performed within weeks of each other. UST imaging was carried out with the SoftVue system (Delphinus Medical Technologies) and the MR exams with a Philips Achieva 3T system. The resulting image sequences were qualitatively and quantitatively to assess imaging performance of UST. As discussed above, UST images correlate best with MR images. Further inspection shows that of the three UST image types, the sound speed image correlates best with MR. **Figure 8** shows a coronal view comparison between UST speed of sound and MR contrast-enhanced fat subtracted images of representative breast parenchyma.

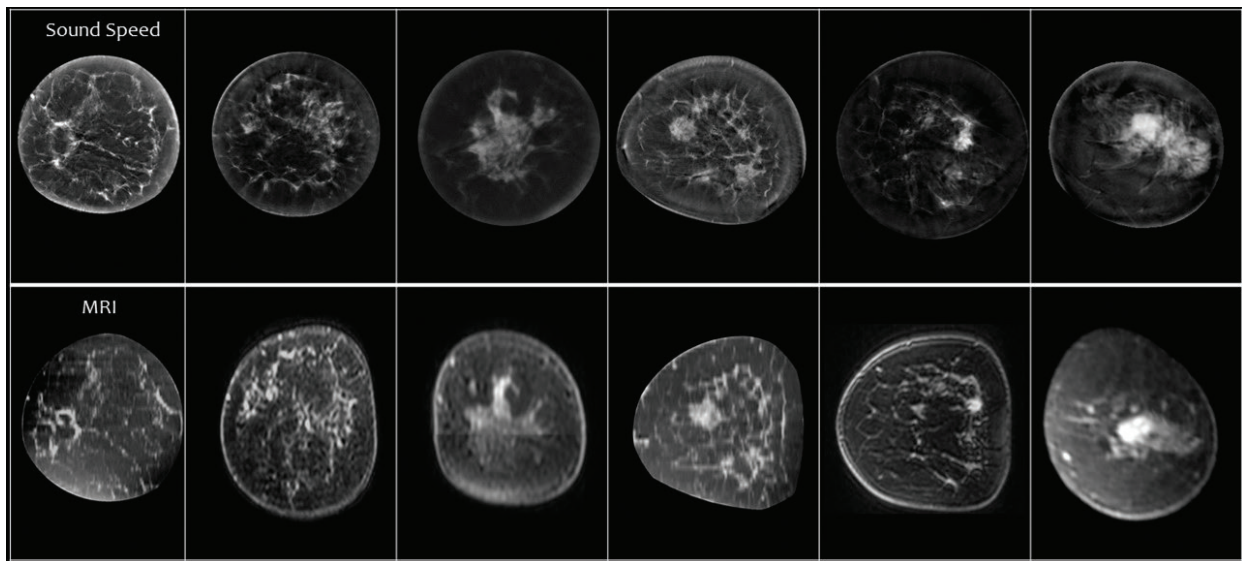


Figure 8. Top: Coronal UST sound speed images for six different patients. Bottom: Corresponding fat subtracted contrast-enhanced MR images.

The parenchymal patterns are very similar with the only major difference relating to the shape of the breast. This difference can be explained by the fact that the SoftVue system utilizes water so that buoyancy foreshortens the breast while with MR, gravity lengthens the breast in the AP dimension (i.e. prone).

As discussed above, UST images correlate best with MR images. Further inspection shows that of the three UST image types, the sound speed image correlates best with MR, as illustrated in **Figure 8**. The parenchymal patterns are very similar with the only major difference relating to the shape of the breast. This difference can be explained by the fact that the SoftVue system utilizes water so that the buoyancy force helps shape the breast while with MR, gravity shapes the breast.

4. Breast volume comparisons

MRI was used as the gold standard for defining the extent of the breast tissue. MRI and UST breast volumes were compared using a paired t-test. In the first step, a k-means segmentation algorithm was applied to T1 breast MR images to automatically separate out the non-tissue background. In the second step, the boundary between the breast tissue and the chest wall was drawn manually and the chest wall removed, leaving behind only breast tissue (**Figure 9**).

In the UST images a semi-automated tool was used to draw a boundary around the breast tissue in each coronal slice and everything outside the boundary removed (water signal). Any slices containing chest wall signal were also removed. The resulting stack of slices then represented the pure breast volume scanned by UST.

The two sets of volumes were plotted against each other as shown in **Figure 10**. The average breast volumes for MRI and UST were compared and the result shown in **Table 2**. As expected, the UST

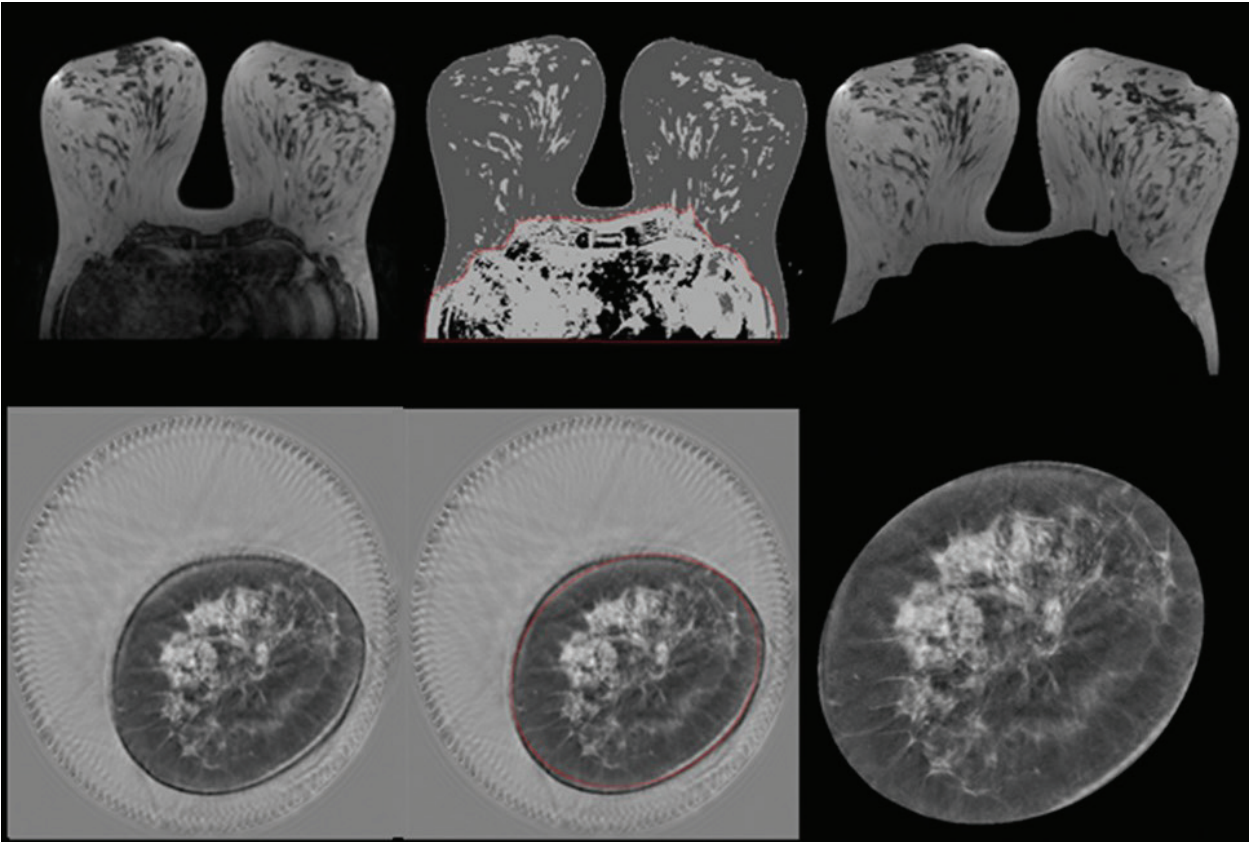


Figure 9. The segmentation process for MR images (top) and UST images (bottom). From left to right, original image, segmentation boundary and the final segmented image.

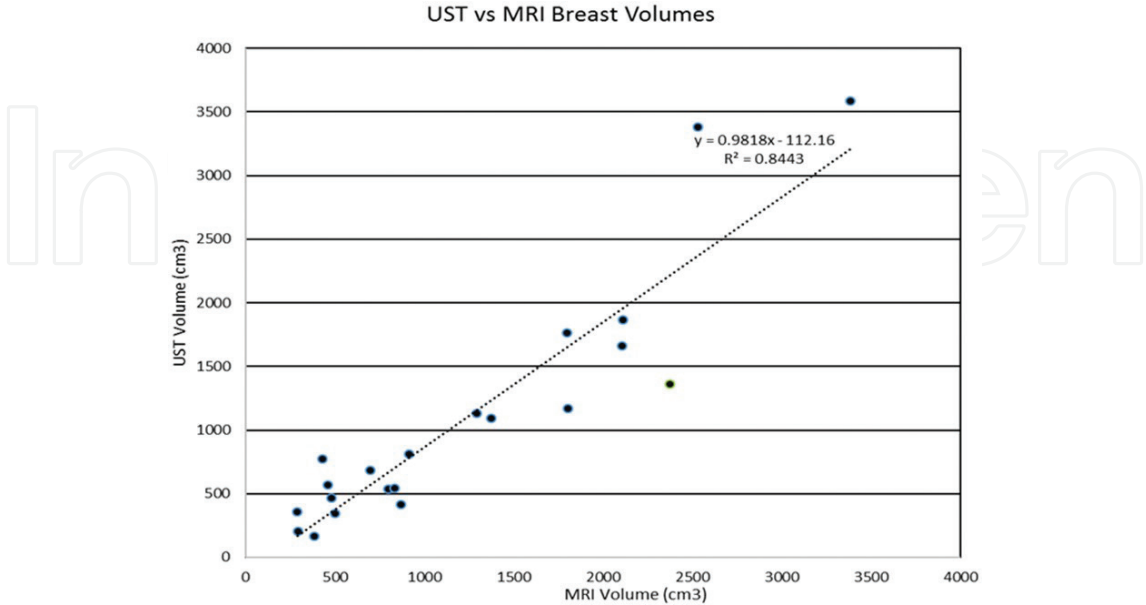


Figure 10. Correlation between UST and MR measured breast volumes.

Mean MRI volume (cm ³)	Mean UST volume (cm ³)	<i>p</i> Value
1224	1089	0.113

Table 2. Volume comparison.

scanned volume was less than that of MRI and was found to be about 89% of the MRI volume on average. However, a student's paired t-test indicates that this difference is not significant. Since UST cannot fully access the axilla, it is likely that the UST scanned volume is somewhat lower than that of MRI, even though UST generally reaches the pectoralis muscle at the chest wall.

5. Spatial resolution assessment

The spatial resolution of each modality was estimated using profile cuts of thin features using, the full-width, half-maximum criterion as shown in **Figure 11**. The results of the spatial resolution analysis are shown in **Table 3**. The spatial resolution was found to be dependent on the reprojection type for both MRI and with UST outperforming MRI in the coronal plane and MRI outperforming UST in the other projections. (However, MR acquisitions with isotropic voxels would show comparable resolution to UST in the coronal plane). The UST image voxels are not isotropic and data acquisition cannot be readily adjusted like MR, such that UST reconstructed in axial and sagittal planes have resolution that approach the 2.5 mm slice thickness at this time.

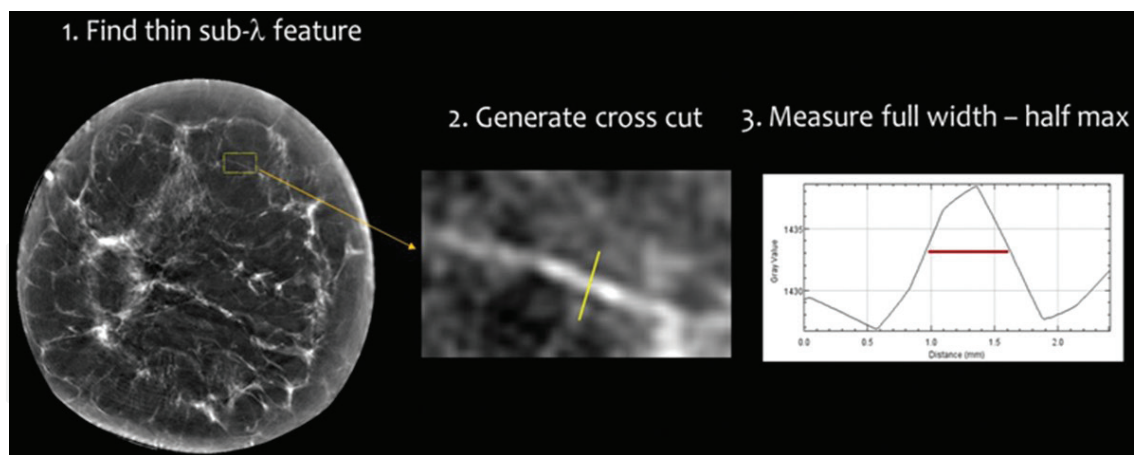


Figure 11. The spatial resolution of each modality was estimated using profile cuts of thin features using, the full-width, half-maximum criterion, as illustrated.

Resolution	UST	MRI
Coronal	0.7 ± 0.1 mm	1.6 ± 0.3 mm
Axial/sagittal	2.5 ± 0.5 mm	0.8 ± 0.1 mm

Table 3. Spatial resolution comparison.

6. Lesion characterization

Ultrasound breast imaging reporting and data system (US-BI-RADS) criteria are predominantly devoted to assessment of tumor shape, margins and interaction with adjacent tissue. However, criteria such as shadowing or enhanced through transmission are not applicable to UST's circular geometry. In addition, UST, operating at 3 MHz, appears more sensitive to the specular reflectors of benign mass capsules, or the spiculations and/or architectural distortions of many cancers. Therefore, we developed a 5-point scale that combined US-BI-RADS criteria for tumor margins, as well as possibilities for peritumoral tissue interaction (**Figure 12**).

Masses were characterized by a (i) Margin Boundary score, (ii) reflectivity, (iii) quantitative SS evaluation and (iv) ATT evaluations. A semi-automatic region-of-interest (ROI) tool was used to determine the quantitative properties of each mass. After identifying the mass of interest, a simple elliptical ROI is drawn around the mass. The ROI algorithm then generates 20 radial ellipsoids – 10 inside and 10 outside the mass. Quantitative information was then measured for each of the 20 annuli for subsequent analysis. The region of interest (ROI) analysis was performed on all identified lesions using all three UST image types. Combinations of the ROI generated values were used to characterize all masses in the study.

Ongoing analyses of the ROI tool have not yet led to full evaluation of second and third-order statistics of textural analyses, as well as their impacts upon decision analysis and predictive values. However, our recent RSNA presentation highlighted the significant impacts of first-order statistics such as standard deviation, within the tumoral ROI and comparisons with the surrounding peritumoral region [69]. Scatterplots and box plots of the optimal methods were used to illustrate the characterization potential. The box plot in **Figure 13** shows the differentiation achieved when using the boundary score (**Figure 6**) combined with the first-order statistic of standard deviation, a more crude measure of heterogeneity, based upon tumoral ROI extracted from ATT images, which had only slightly higher significance than SS [69]. These ROIs were again obtained by simply drawing an elliptical ROI around the mass and determining the standard deviation within the ROI. The box plot was based on taking the average values for 107 benign lesions and 31 cancers [69].

Upon further investigation, it was found that the SS of the peritumoral mass region (defined by an annular area just outside the mass boundary ROI) further separated the benign masses from cancer. A scatter plot based on all of these parameters is shown in **Figure 14**. The scatter plot shows separately the cancers, fibroadenomas and cancers. The cancers are tightly

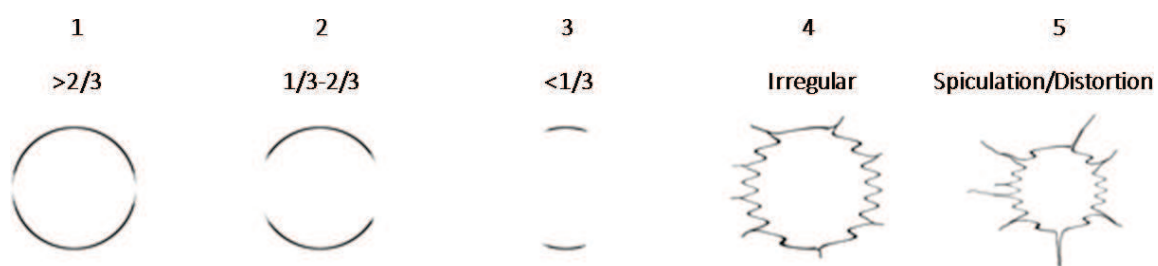


Figure 12. Schematic of shape and margin analysis and associated grading scheme.

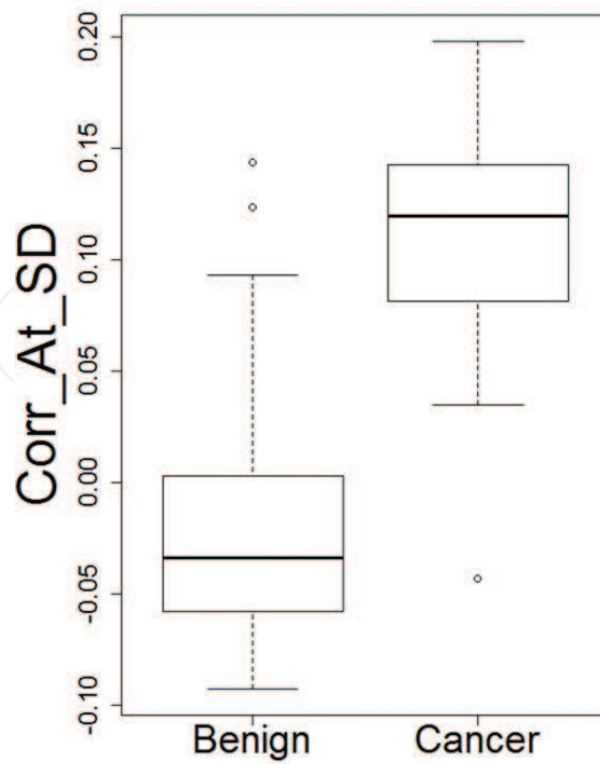


Figure 13. Separation of cancer from benign when using boundary score and heterogeneity score.

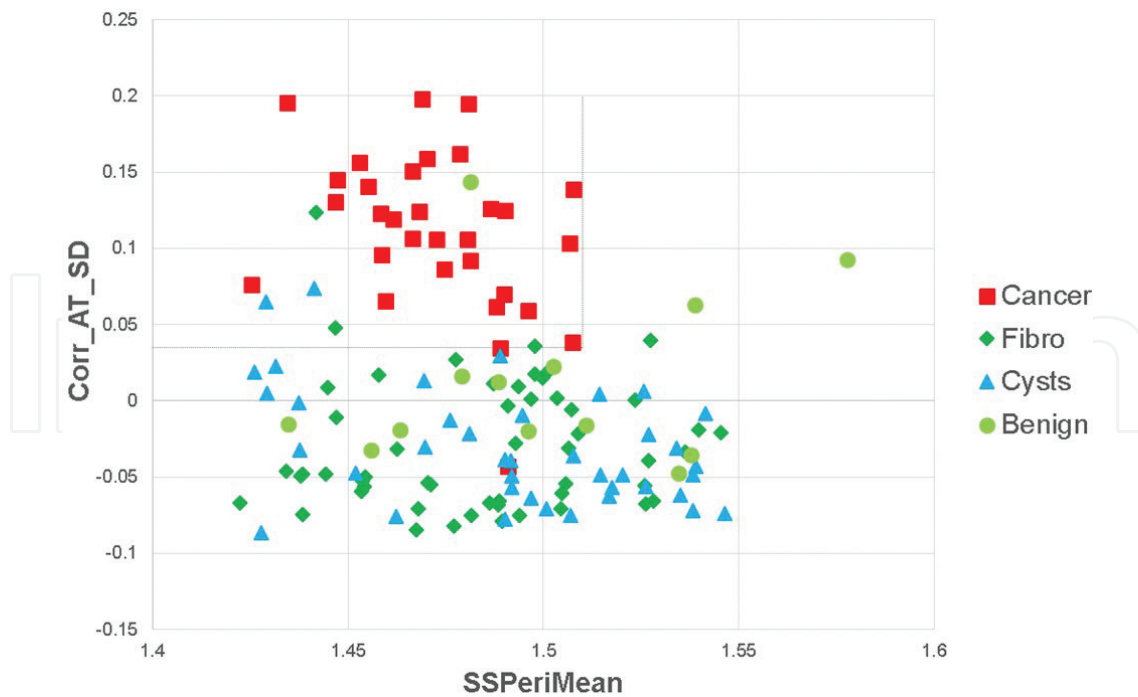


Figure 14. Scatter plot showing the distribution of cancers (squares), Fibroadenomas (diamonds), cysts (triangles) and other benign (circles).

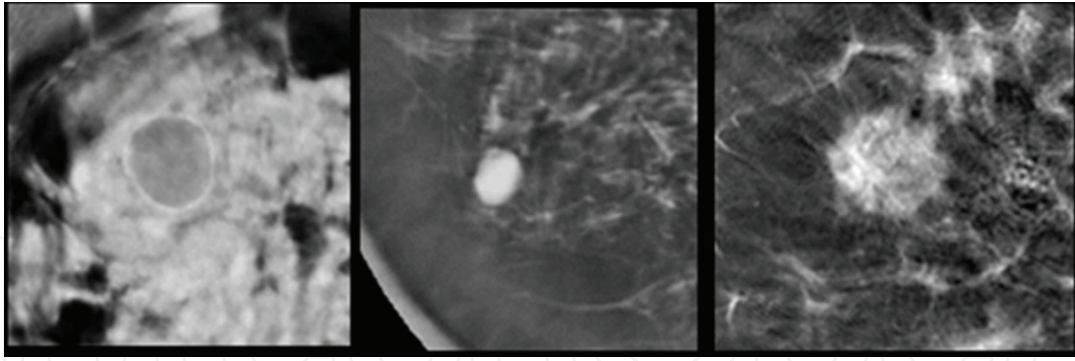


Figure 15. Cyst, fibroadenoma, cancer: Waveform SS images showing well circumscribed margins and smooth internal textures for both the 1.5 cm cyst in dense white breast tissue (left) and the 0.7 cm fibroadenoma (middle) in darker fat. The 1.8 cm cancer (right) has irregular margins, heterogeneous content and subtle peritumoral spiculations.

grouped in the top left corner of the plot indicating high boundary scores, high heterogeneity and lower peritumoral sound speed. By these measures, there was not much separation between cysts and fibroadenomas but significant separation between them and cancer. ROC analysis of the data represented in the scatter plot indicates a PPV of 91% when the sensitivity is 97%. However, this is a subset of data relative to an expanded ongoing study that includes more quantitative margin analyses. The ultimate goal is to generate textural analyses that will be less operator dependent and serve as appropriate diagnostic aids for a detected mass by simply requiring the radiologist to draw an ellipsoidal ROI. This method can also serve as a teaching tool for identifying grossly apparent textural differences within the tumor and surrounding peritumoral region. **Figure 15** shows the basic differences in sound speed texture noted for many cysts, fibroadenomas and cancer.

7. Conclusions

In this study we reviewed the status of breast cancer screening and the potential role that ultrasound tomography (UST) could play in breast imaging. Several results from recent ongoing UST studies were used in this review. The main conclusions from those studies are:

- (i) UST sound speed demonstrated a high degree of correlation of breast tissue structures relative to fat subtracted contrast-enhanced MRI. This correlation of structures was most evident in the coronal plane comparisons.
- (ii) UST can scan ~90% of the volume of the breast compared to MRI. With proper positioning UST can image the pectoralis muscle and a portion of the axillary tissue.
- (iii) UST demonstrated a spatial resolution of 0.7mm in the coronal plane, similar to MRI.
- (iv) Initial clinical results suggest an ability to characterize lesions using margin boundary scores in combination with sound speed and attenuation parameters. These parameters leverage all three imaging modes of UST (reflection, sound speed and attenuation).

UST is a promising new modality that has the potential to complement existing breast imaging methods to aid in lesion detection and characterization. Future larger scale studies will assess UST's role in diagnostic and screening settings.

Acknowledgements

The authors thank Dr. Mark Sak for providing images relating to the MRI comparison study and Mr. Mark Krycia for his help in the statistical analysis of the lesion characterization data. The work presented in this paper was supported by NIH grant 5R44CA165320-05.

Author details

Nebojsa Duric^{1*} and Peter Littrup²

*Address all correspondence to: duric@karmanos.org

1 Karmanos Cancer Institute, Wayne State University, Detroit, MI, USA

2 Crittenton Hospital, Troy, MI, USA

References

- [1] Surveillance, Epidemiology, and End Results Program. Available from: <http://seer.cancer.gov/>
- [2] American Cancer Society. Cancer Prevention & Early Detection Facts & Figures 2009. Atlanta, GA: American Cancer Society; 2009. pp. 34-37
- [3] Ernster VL, Barclay J, Kerlikowske K, Wilkie H, Ballard-Barbash R. Mortality among women with ductal carcinoma in situ of the breast in the population-based surveillance, epidemiology and end results program. *Archives of Internal Medicine*. 2000;**160**(7): 953-958
- [4] Chen TH, Yen AM, Fann JC, Gordon P, Chen SL, Chiu SY, Hsu CY, Chang KJ, Lee WC, Yeoh KG, Saito H, Promthet S, Hamashima C, Maidin A, Robinson F, Zhao LZ. Clarifying the debate on population-based screening for breast cancer with mammography: A systematic review of randomized controlled trials on mammography with Bayesian meta-analysis and causal model. *Medicine (Baltimore)*. 2017;**96**:e5684
- [5] Boyd NF, Guo H, Martin LJ, Sun L, Stone J, Fishell E, Jong RA, Hislop G, Chiarelli A, Minkin S, et al. Mammographic density and the risk and detection of breast cancer. *The New England Journal of Medicine*. 2007;**356**:227-236
- [6] Chen J, Pee D, Ayyagari R, Graubard B, Schairer C, Byrne C, Benichou J, Gail MH. Projecting absolute invasive breast cancer risk in white women with a model that includes mammographic density. *Journal of the National Cancer Institute*. 2006;**98**:1215-1226

- [7] Ursin G, Hovanesian-Larsen L, Parisky YR, Pike MC, Wu AH. Greatly increased occurrence of breast cancers in areas of mammographically dense tissue. *Breast Cancer Research*. 2005;**7**:R605-R608
- [8] Martin LJ, Boyd N. Potential mechanisms of breast cancer risk associated with mammographic density: Hypotheses based on epidemiological evidence. *Breast Cancer Research*. 2008;**10**:1-14
- [9] Armstrong K, Moye E, Williams S, Berlin JA, Reynolds EE. Screening mammography in women 40 to 49 years of age: A systematic review for the American College of Physicians. *Annals of Internal Medicine*. 2007;**146**:516-526
- [10] Breast Cancer Screening (PDQ®)—Health Professional Version. <http://www.cancer.gov/cancertopics/pdq/screening/breast/healthprofessional/page7>
- [11] Friedewald SM, Rafferty EA, Rose SL, Durand MA, Plecha DM, Greenberg JS, Hayes MK, Copit DS, Carlson KL, Cink TM, Barke LD, Greer LN, Miller DP, Conant EF. Breast cancer screening using tomosynthesis in combination with digital mammography. *Journal of the American Medical Association*. 2014;**311**(24):2499-2507
- [12] Hendrick RE. Radiation doses and cancer risks from breast imaging *Radiology*. 2010;**257**(1):246-253
- [13] Turnbull LW. Dynamic contrast-enhanced MRI in the diagnosis and management of breast cancer. *Journal of Biomolecular NMR*. 2008
- [14] Jansen SA, Fan X, Karczmar GS, Abe H, Schmidt RA, Newstead GM. Differentiation between benign and malignant breast lesions detected by bilateral dynamic contrast-enhanced MRI: A sensitivity and specificity study. *Magnetic Resonance in Medicine*. 2008;**59**(4):747. John Wiley & Sons, Ltd
- [15] Kuhl CK, Schrading S, Bieling HB, Wardelmann E, Leutner CC, Koenig R, Kuhn W, Schild HH. MRI for diagnosis of pure ductal carcinoma in situ: A prospective observational study. *The Lancet*. 2007;**370**:485-492
- [16] Saslow D, Boetes C, Burke W, Harms S, Leach MO, Lehman CD, Morris E, Pisano E, Schnall M, Sener S, Smith RA, Warner E, Yaffe M, Andrews KS, Russell CA; American Cancer Society Breast Cancer Advisory Group. American Cancer Society guidelines for breast screening with MRI as an adjunct to mammography. *CA: A Cancer Journal for Clinicians*. 2007;**57**:75-89
- [17] Chen JH, et al. MRI evaluation of pathologically complete response and residual tumors in breast cancer after neoadjuvant chemotherapy. *Cancer*. 2008;**112**(1):17-26
- [18] Sharma U, et al. Longitudinal study of the assessment by MRI and diffusion-weighted imaging of tumor response in patients with locally advanced breast cancer undergoing neoadjuvant chemotherapy. *NMR in Biomedicine*. 2009;**22**(1):104-113
- [19] Bando H, et al. Imaging evaluation of pathological response in breast cancer after neoadjuvant chemotherapy by real-time sonoelastography and MRI. *European Journal of Cancer-Supplement*. 2008;**6**(7):66-66

- [20] Bhattacharyya M, et al. Using MRI to plan breast-conserving surgery following neoadjuvant chemotherapy for early breast cancer. *British Journal of Cancer*. 2008;**98**(2): 289-293
- [21] Partridge S. Recurrence rates after DCE-MRI image guided planning for breast-conserving surgery following neoadjuvant chemotherapy for locally advanced breast cancer patients. *Breast Diseases: A Year Book Quarterly*. 2008;**19**(1):91-91
- [22] Tozaki M. Diagnosis of breast cancer: MDCT versus MRI. *Breast Cancer*. 2008;**15**(3):205-211
- [23] Partridge S, et al. Accuracy of MR imaging for revealing residual breast cancer in patients who have undergone neoadjuvant chemotherapy. *American Roentgen Ray Society*. 2002;**172**:1193-1199
- [24] Brem RF, Tabár L, Duffy SW, Inciardi MF, Guingrich JA, Hashimoto BE, Lander MR, Lapidus RL, Peterson MK, Rapelyea JA, Roux S, Schilling KJ, Shah BA, Torrente J, Wynn RT, Miller DP. Assessing improvement in detection of breast cancer with three-dimensional automated breast US in women with dense breast tissue: The SonoInsight Study. *Radiology*. 2015 Mar;**274**(3):663-673
- [25] Berg WA, Zhang Z, Lehrer D, Jong RA, Pisano ED, Barr RG, Böhm-Vélez M, Mahoney MC, Evans WP 3rd, Larsen LH, Morton MJ, Mendelson EB, Farria DM, Cormack JB, Marques HS, Adams A, Yeh NM, Gabrielli G; ACRIN 6666 Investigators. Detection of breast cancer with addition of annual screening ultrasound or a single screening MRI to mammography in women with elevated breast cancer risk. *Journal of the American Medical Association*. 2012 Apr 4;**307**(13):1394-1404
- [26] Hooley RJ, Greenberg KL, Stackhouse RM, Geisel JL, Butler RS, Philpotts LE. Screening US in patients with mammographically dense breasts: Initial experience with Connecticut Public Act 09-41. *Radiology*. 2012 Oct;**265**(1):59-69
- [27] Kelly KM, Dean J, Comulada WS, Lee SJ. Breast cancer detection using automated whole breast ultrasound and mammography in radiographically dense breasts. *European Radiology*. 2010 Mar;**20**(3):734-742
- [28] Corsetti V, Houssami N, Ferrari A, Ghirardi M, Bellarosa S, Angelini O, Bani C, Sardo P, Remida G, Galligioni E, Ciatto S. Breast screening with ultrasound in women with mammography-negative dense breasts: Evidence on incremental cancer detection and false positives, and associated cost. *European Journal of Cancer*. 2008 Mar;**44**(4):539-544
- [29] Crystal P, Strano SD, Shcharynski S, Koretz MJ. Using sonography to screen women with mammographically dense breasts. *American Journal of Roentgenology*. 2003 Jul;**181**(1):177-182
- [30] Leconte I, Feger C, Galant C, Berlière M, Berg BV, D'Hoore W, Maldague B. Mammography and subsequent whole-breast sonography of non palpable breast cancers: The importance of radiologic breast density. *American Journal of Roentgenology*. 2003 Jun;**180**(6):1675-1679

- [31] Kolb TM, Lichy J, Newhouse JH. Comparison of the performance of screening mammography, physical examination, and breast US and evaluation of factors that influence them: An analysis of 27,825 patient evaluations. *Radiology*. 2002 Oct;**225**(1):165-175
- [32] Kaplan SS. Clinical utility of bilateral whole-breast US in the evaluation of women with dense breast tissue. *Radiology*. 2001 Dec;**221**(3):641-649
- [33] Buchberger W, Niehoff A, Obrist P, DeKoekkoek-Doll P, Dünser M. Clinically and mammographically occult breast lesions: Detection and classification with high-resolution sonography. *Seminars in ultrasound, CT, and MR*. 2000 Aug;**21**(4):325-336
- [34] Gordon PB, Goldenberg SL. Malignant breast masses detected only by ultrasound. A retrospective review. *Cancer*. 1995 Aug 15;**76**(4):626-630
- [35] Ernster VL, Ballard-Barbash R, Barlow WE, Zheng Y, Weaver DL, et al. Detection of ductal carcinoma *in situ* in women undergoing screening mammography. *Journal of the National Cancer Institute*. 2002;**94**:1546-1554
- [36] Johnson S, et al. From laboratory to clinical trials: An odyssey of ultrasound inverse scattering imaging for breast cancer diagnosis. *The Journal of the Acoustical Society of America*. 2006;**120**:3023
- [37] Johnson SA and Tracy ML. Inverse scattering solutions by a sinc basis, multiple source, moment method. Part I: Theory, *Ultrasonic Imaging*. 1983;**5**:361-375
- [38] Schreiman JS, Gisvold JJ, Greenleaf JF, Bahn RC. Ultrasound transmission computed tomography of the breast. *Radiology*. 1984;**150**:523-530
- [39] Natterer FA. Propagation backpropagation method for ultrasound tomography. *Inverse Problems*. 1995;**11**:1225-1232
- [40] Carson PL, Meyer CR, Scherzinger AL, Oughton TV. Breast imaging in coronal planes with simultaneous pulse echo and transmission ultrasound. *Science*. 1981 Dec 4;**214**(4525):1141-1143
- [41] Andre MP, Janee HS, Martin PJ, Otto GP, Spivey BA, Palmer DA. High-speed data acquisition in a diffraction tomography system employing large-scale toroidal arrays. *International Journal of Imaging Systems and Technology*. 1997;**8**:137-147
- [42] Johnson SA, Borup DT, Wiskin JW, Natterer F, Wuebbeling F, Zhang Y, Olsen C. Apparatus and Method for Imaging with Wavefields using Inverse Scattering Techniques. United States Patent 6,005,916; 1999
- [43] Marmarelis VZ, Kim T, Shehada RE. Proceedings of the SPIE: Medical Imaging 2003; San Diego, California; Feb 23-28, 2002. *Ultrasonic Imaging and Signal Processing – Paper 5035-6*
- [44] Liu DL, Waag RC. Propagation and backpropagation for ultrasonic wavefront design. *IEEE Transactions on Ultrasonics, Ferroelectrics, and Frequency Control*. 1997;**44**(1):1-13

- [45] Liu D, Waag R. Harmonic amplitude distribution in a wideband ultrasonic wavefront after propagation through human abdominal wall and breast specimens. *The Journal of the Acoustical Society of America*. 1997;**101**:1172
- [46] Duric N, Littrup PJ, Poulo L, et al. Detection of breast cancer with ultrasound tomography: First results with the computed Ultrasound Risk Evaluation (UST) prototype. *Medical Physics*. 2007;**34**:773-785
- [47] Boyd NF, et al. Breast tissue composition and susceptibility to breast cancer. *JNCI: Journal of the National Cancer Institute (0027-8874)*. 2010;**102**(16):1224. (Review Article)
- [48] Glide C, Duric N, Littrup P. Novel approach to evaluating breast density utilizing ultrasound tomography. *Medical Physics*. 2007;**34**(2):744-753
- [49] Glide-Hurst CK, Duric N, Littrup P. Volumetric breast density evaluation from ultrasound tomography images. *Medical Physics*. 2008;**35**(9):3988-3997
- [50] Myc L, Duric N, Littrup P, Li C, Ranger B, Lupinacci J, Schmidt S, et al. Volumetric breast density evaluation by Ultrasound Tomography and Magnetic Resonance Imaging: A preliminary comparative study. *Proceedings of SPIE*. 2010;**7629**:76290N
- [51] Li C, Duric N, Huang L. Clinical breast imaging using sound-speed reconstructions of ultrasound tomography data. *Proceedings of SPIE*. 2008;**6920**:6920-69309
- [52] Li C, Duric N, Huang L. Comparison of ultrasound attenuation tomography techniques for breast cancer diagnosis. *Proceedings of SPIE*. 2008;**6920**:6920-6949
- [53] Li C, Huang L, Duric N, Zhang H, Rowe C. An improved automatic time-of-flight picker for medical ultrasound tomography. *Ultrasonics*. (Accepted)
- [54] Duric N, Littrup P, Li C, Rama O, Bey-Knight L, Schmidt S, Lupinacci J. Detection and characterization of breast masses with ultrasound tomography: Clinical results. *Proceedings of SPIE: Medical Imaging*. 2009;**7265**:72651G-1-8
- [55] Simonetti F, Huang L, Duric N. A multiscale approach to diffraction tomography of complex three-dimensional objects. *Applied Physics Letters (0003-6951)*. 2009;**95**(6):061904
- [56] Simonetti F, Huang L, Duric N, Littrup P. Diffraction and coherence in breast ultrasound tomography: A study with a toroidal array. *Medical Physics*. 2009;**36**(7):2955-2965
- [57] Duric N, Littrup P, Chandiwala-Mody P, Li C, Schmidt S, et al. In-vivo imaging results with ultrasound tomography: Report on an ongoing study at the Karmanos Cancer Institute. *Proceedings of SPIE*. 2010;**7629**:76290M
- [58] Ranger B, Littrup P, Duric N, Li C, Lupinacci J, Myc L, Rama O, Bey-Knight L. Breast imaging with acoustic tomography: A comparative study with MRI. *Proceedings of SPIE: Medical Imaging*. 2009;**7265**:726510-1-8
- [59] Ranger B, Littrup P, Duric N, Li C, Schmidt S, et al. Breast imaging with ultrasound tomography: A comparative study with MRI. *Proceedings of SPIE*. 2010;**7629**:76291C

- [60] Ranger B, Littrup PJ, Duric N, Chandiwala-Mody P, Li C, Schmidt S, Lupinacci J. Breast ultrasound tomography versus magnetic resonance imaging for clinical display of anatomy and tumor rendering: Preliminary results. *American Journal of Roentgenology*. 2012;**198**(1):233
- [61] Schmidt S, Huang Z, Duric N, Li C, Roy O. Modification of Kirchhoff migration with variable sound speed and attenuation for acoustic imaging of media and application to tomographic imaging of the breast. *Medical Physics*. 2011;**38**:998
- [62] Entrekin RR, Porter BA, Sillesen HH, Wong AD, Cooperberg PL, Fix CH. Real-time spatial compound imaging application to breast, vascular, and musculoskeletal ultrasound. *Seminars in Ultrasound, CT, and MR*. 2001;**22**:50-64
- [63] Stavros AT, Thickman D, Rapp CL, Dennis MA, Parker SH, Sisney G. Solid breast nodules: Use of sonography to distinguish between benign and malignant lesions. *Radiology*. 1995;**196**(1):123-134
- [64] Greenleaf JF, Johnson SA, Bahn RC, Rajagopalan B. Quantitative cross-sectional imaging of ultrasound parameters. 1977 *Ultrasonics Symposium Proc., IEEE Cat. # 77CH1264-1SU*; 1977. pp. 989-995
- [65] Goss SA, Johnston RL and Dunn F. Comprehensive compilation of empirical ultrasonic properties of mammalian tissues. *The Journal of the Acoustical Society of America*. 1978;**64**:423-457
- [66] Duck FA. *Physical Properties of Tissue*. London: Academic Press; 1990
- [67] Edmonds PD, Mortensen CL, Hill JR, Holland SK, Jensen JF, Schattner P, Valdes AD. Ultrasound tissue characterization of breast biopsy specimens. *Ultrasound Imaging*. 1991;**13**:162-185
- [68] Weiwad W, Heinig A, Goetz L, Hartmann H, Lampe D, Buchman J, et al. Direct measurement of sound velocity in various specimens of breast tissue. *Investigative Radiology*. 2000;**35**:721-726
- [69] Littrup PJ, Duric N, Brem RF, Yamashita MW. Improving specificity of whole breast ultrasound using tomographic techniques. Paper SSA02-05. Presented at Radiology Society of North America, Nov 27, 2016

